Published in final edited form as:
Biochim Biophys Acta. 2011 April ; 1808(4): 1072–1080. doi:10.1016/j.bbamem.2010.12.019.

The immiscible cholesterol bilayer domain exists as an integral part of phospholipid bilayer membranes

Marija Raguz[a,b], **Laxman Mainali**[a], **Justyna Widomska**[c], and **Witold K. Subczynski**[a,*]

[a] Department of Biophysics, Medical College of Wisconsin, Milwaukee, WI 53226, USA [b] Department of Medical Physics and Biophysics, School of Medicine, University of Split, Split, Croatia [c] Department of Biophysics, Medical University, Lublin, Poland

Abstract

Electron paramagnetic resonance (EPR) spin-labeling methods were used to study the organization of cholesterol and phospholipids in membranes formed from Chol/POPS (cholesterol/1-palmitoyl-2-oleoyl-*sn*-glycero-3-phosphatidylserine) mixtures, with mixing ratios from 0 to 3. It was confirmed using the discrimination by oxygen transport and polar relaxation agent accessibility methods that the immiscible cholesterol bilayer domain (CBD) was present in all of the suspensions when the mixing ratio exceeded the cholesterol solubility threshold (CST) in the POPS membrane. The behavior of phospholipid molecules was monitored with phospholipid analogue spin labels (n-PCs), and the behavior of cholesterol was monitored with the cholesterol analogue spin labels CSL and ASL. Results indicated that phospholipid and cholesterol mixtures can form a membrane suspension up to a mixing ratio of ~2. Additionally, EPR spectra for n-PC, ASL, and CSL indicated that both phospholipids and cholesterol exist in these suspensions in the lipid-bilayer-like structures. EPR spectral characteristics of n-PCs (spin labels located in the phospholipid cholesterol bilayer, outside the CBD) change with increase in the cholesterol content up to and beyond the CST. These results present strong evidence that the CBD forms an integral part of the phospholipid bilayer when formed from a Chol/POPS mixture up to a mixing ratio of ~2. Interestingly, CSL in cholesterol alone (without phospholipids) when suspended in buffer does not detect formation of bilayer-like structures. A broad, single-line EPR signal is given, similar to that obtained for the dry film of cholesterol before addition of the buffer. This broad, single-line signal is also observed in suspensions formed for Chol/POPS mixtures (as a background signal) when the Chol/POPS ratio is much greater than 3. It is suggested that the EPR spin-labeling approach can discriminate and characterize the fraction of cholesterol that forms the CBD within the phospholipid bilayer.

Keywords

cholesterol bilayer domain; lens lipids; cholesterol; membrane; spin label; EPR

[*]CORRESPONDING AUTHOR: Witold K. Subczynski, Department of Biophysics, Medical College of Wisconsin, 8701 Watertown Plank Road, Milwaukee, WI 53226, USA, Tel: (414) 456-4038, Fax: (414) 456-6512, subczyn@mcw.edu.

1. Introduction

Fiber cell membranes—which build the human eye lens—are overloaded with cholesterol, which saturates the phospholipid bilayer and also leads to the formation of immiscible cholesterol bilayer domains (CBDs). Their appearance is usually a sign of pathology [1]. However, in the eye lens, CBDs play a positive physiological role, maintaining lens transparency [2–4] and possibly protecting against cataract formation [2,5]. Better understanding of the physiological functions of cholesterol and the CBD requires improved knowledge of cholesterol function on a molecular level. These functions are shown by cholesterol-induced changes in the properties of the lipid bilayer portion of the fiber-cell plasma membrane. We investigated the bulk properties of the phospholipid cholesterol domain (PCD; the phospholipid cholesterol membrane saturated with cholesterol before formation of the CBD, or the phospholipid cholesterol domain coexisting with the CBD) in lens lipid membranes from different animals [6–8], from animals at different ages [6,7,9], and from different eye regions [9]. The phospholipid composition of the fiber-cell membrane significantly changes between species [10], with age [11], and also between different regions of the lens [12]. Surprisingly, independent of these differences, profiles of bulk membrane properties were nearly identical in all of the investigated membranes. We conclude that *the saturating content of cholesterol in the fiber-cell membrane keeps the physical properties of the PCD in the lipid-bilayer portion of the membrane consistent and independent of changes in the phospholipid composition.* The profiles mentioned above were also very similar to those in membranes in which the CBD was already formed—thus, in the PCD surrounding the CBD [8,9]. We conclude further that *the CBD has some function specific to the fiber-cell membrane. The CBD provides buffering capacity for cholesterol concentration in the surrounding phospholipid bilayer, keeping it at a constant saturating level, and thus keeping the physical properties of the membrane independent of changes in the phospholipid composition.* These results are significant for human lenses where changes in lens phospholipid composition are most pronounced [13].

Differential scanning calorimetry (DSC) [14–16], X-ray or neutron diffraction [2,14,15,17,18], and magic-angle-spinning nuclear magnetic resonance (MAS NMR) [16,19] have been mainly applied to detect and investigate cholesterol crystals in model membranes. These techniques show that in suspensions of cholesterol and phospholipid mixtures with a Chol/PL molar ratio above the cholesterol solubility threshold (CST), cholesterol molecules are found in one of three previously characterized triclinic crystal structures depending on the state of hydration and temperature [20]. The consensus in the literature is that the structure of these crystals (with a pseudo-bilayer structure and a bilayer thickness of 34 Å) is the same as the structure of the CBD. Recently, we used the EPR discrimination by oxygen transport (DOT) method to detect the CBD in lipid bilayer membranes and to evaluate oxygen transport across the domain [8,9]. EPR spin-labeling methods also make it possible to obtain molecular-level information on the organization and dynamics of cholesterol molecules in the CBD as well as information on some physical properties of this domain. Results presented here point out significant differences between organization of cholesterol in CBDs and in cholesterol crystals.

Cholesterol crystals have been observed in fiber-cell membranes from normal and cataractous lenses by X-ray diffraction [2,4,5]. However, none of the experimental techniques presented above have provided strong evidence that they exist as an integral part of the phospholipid bilayer [21]. Based on X-ray diffraction data for intact membranes [2] and DSC measurements in model membranes [22–24], it is suggested that cholesterol crystals are in “intimate contact” with phospholipids and are possibly not present as morphologically separate structures. Due to these uncertainties, we have undertaken additional effort to provide definitive proof for our hypothesis that the CBD is formed

within the PCD. For these investigations, we chose 1-palmitoyl-2-oleoyl-*sn*-glycero-3-phosphatidylserine (POPS) because of the low CST in its membrane [14,21,25,26].

There are three possible cases for CBD formation in membranes. First, the CBD can be formed as an integral part of the phospholipid bilayer (Fig. 1A). In this case, phospholipid molecules and phospholipid analogue spin labels should only be located in the PCD, while cholesterol molecules and cholesterol analogue spin labels are distributed between both domains. Second, the CBD can be formed as a separate entity outside of the PCD (Fig. 1B). The distribution of molecules should be similar to the first case. However, cholesterol molecules cannot freely diffuse from one domain to the other. Third, when the CBD is formed as an integral part of the phospholipid bilayer, some parts of cholesterol form separate, ill-defined structures outside the lipid bilayer (Fig.1C). It is likely that these structures are cholesterol crystals, as detected by the DSC and X-ray diffraction methods [21,24,27]. Only in the second case should the presence of the CBD not affect the properties of the separately existing PCD. Figure 1 presents the guidelines for planning experiments and interpreting results.

2. Materials and methods

2.1. Materials

One-palmitoyl-2-(n-doxylstearoyl)phosphatidylcholine spin labels (n-PC, n= 5, 14, and 16), cholesterol, and phospholipids were obtained from Avanti Polar Lipids, Inc. (Alabaster, AL). Cholesterol analogues, androstane spin label (ASL), and cholestane spin label (CSL) were purchased from Molecular Probes (Eugene, OR). Other chemicals (of at least reagent grade) were purchased from Sigma-Aldrich (St. Louis, MO).

2.2. Preparation of lipid suspensions for measurements of the EPR signal intensity

Either a chloroform solution of POPS containing 1 mol% of 5-, 14-, or 16-PC was mixed with a chloroform solution of cholesterol (without spin label), or a chloroform solution of cholesterol containing 1 mol% of CSL or ASL was mixed with a chloroform solution of POPS (without spin label). After mixing the appropriate amounts of lipids, the chloroform was evaporated under a stream of nitrogen gas, and the lipid film on the bottom of the test tube was thoroughly dried under reduced pressure (about 0.1 mm Hg) for 12 h. In this paper, we use the term “mixing ratio” to indicate the input molar ratio of cholesterol and phospholipids in the lipid mixture, which can be quite different from molar ratios in certain membrane domains after liposome preparation. A buffer solution (0.4 mL of 10 mM PIPES and 150 mM NaCl; pH 7.0) was added to the dried lipids at a temperature above the phase transition (40°C was usually sufficient). According to Dr. Jimmy B. Feix’s suggestion, we used plastic Eppendorf microfuge tubes to avoid electrostatic attachment of lipids to the glass surface. Some lipids cannot be completely detached from glass surfaces. The sample in the microfuge tube was put through five freeze-thaw cycles (liquid nitrogen and ~70°C water) to ensure complete detachment of lipids from the surface. After vigorous vortexing, a sample of the suspension was transferred to a calibrated pipette (50 μL; Drummond Scientific Company, Broomall, PA) just after preparation, without any centrifugation, and used for EPR measurements. Great care was taken to avoid liposome sedimentation. The EPR signal was measured a few times to ensure it did not change in time. In parallel experiments, liposome suspensions were kept in horizontally oriented pipettes for a few hours, allowing liposomes to attach to a glass surface, which protected them from sedimentation. After the liposome suspension was formed and removed, the bottoms of the test tubes were rinsed with 0.5 mL of chloroform to determine if a lipid residue (EPR signal in chloroform) was present.

2.3. Preparation of lipid suspensions for measurement of membrane properties

For measurement of membrane properties, the lipid suspension (multilamellar liposomes) was centrifuged briefly, which significantly increased the signal-to-noise ratio. The loose pellet (about 20% lipids, w/w) was transferred to a 0.6 mm i.d. capillary made of gas-permeable methylpentene polymer (TPX) [28], which was used for conventional and saturation-recovery EPR measurements.

2.4. EPR measurements

EPR spectra were obtained with a Bruker EMX X-band spectrometer using a modulation amplitude of 1.0 G and an incident microwave power of 5.0 mW. The amount of phospholipids and cholesterol in the suspension was expected to be proportional to the EPR signal intensities for 5-PC and CSL, respectively, and was measured as a product of signal amplitude and square of the linewidth of the central line (experiments described in Sect. 3.1). All EPR measurements were performed at 25°C, with the exception of polarity measurements. In these measurements, we used the *z*-component of the hyperfine interaction tensor, A_Z, for 5-PC, ASL, and CSL in the membrane, determined directly from EPR spectra for samples frozen at about −165°C, and recorded with a modulation amplitude of 2.0 G and an incident microwave power of 2.0 mW [14]. With an increase in local polarity, A_Z increased.

The spin-lattice relaxation times, T_1, of spin-labels were determined by analyzing the saturation-recovery signal of the central line obtained by short-pulse saturation-recovery EPR at X-band [29–31]. The concentration of oxygen in the sample was controlled by equilibration with the same gas that was used for the temperature control (i.e., a controlled mixture of nitrogen and dry air adjusted with flowmeters [Matheson Gas Products, Model No. 7631H-604]) [32,33]. Accumulations of the decay signals were carried out with 2048 data points on each decay. The saturation-recovery spectrometer used in these studies was described previously [31,34].

When the Chol/POPS mixing ratio exceeded the CST (33 mol%), the presence of the CBD in the lipid suspension was confirmed using the saturation-recovery EPR technique and the DOT method [35]. As described previously for lens lipid membranes, the cholesterol analogue spin label, ASL, was used to discriminate the CBD and PCD [8,9].

In an analogy to the oxygen transport parameter [36], the relaxation agent accessibility parameter, $P(x)$, for a water-soluble relaxation agent, nickel(II) ethylenediaminediacetic acid (NiEDDA), was defined as:

$$P(x)=T_1^{-1}(20\ \text{mM NiEDDA}, x) - T_1^{-1}(\text{No NiEDDA}, x) \quad (1)$$

This NiEDDA accessibility parameter is proportional to the product of the local concentration and the local translational diffusion coefficient of NiEDDA at the membrane depth “x,” at which the nitroxide moiety is located. Greater P(x) values indicate a greater extent of NiEDDA penetration into the membrane. All accessibility measurements have to be performed for deoxygenated samples. The NiEDDA concentration in buffer is 20 mM. The NiEDDA accessibility parameter and the cholesterol analog spin label, CSL, were used to discriminate the CBD and PCD. Also, the NiEDDA accessibility parameter was measured for 5-PC to confirm changes in local polarity in the PCD induced by the presence of the CBD.

3. Results

3.1. Suspensions made of Chol/POPS mixtures

In these studies, lipid suspensions were formed (as described in Sect. 2.2) from different amounts of cholesterol and POPS. Cholesterol mixing ratios in these preparations varied from 0 to 3. Using the method described in Sect. 2.4, we evaluated the amount of POPS and cholesterol in these suspensions from the EPR signal intensities for 5-PC and CSL, respectively. Results are presented in Fig. 2, where normalized EPR signal intensities for 5-PC and CSL are plotted as a function of the Chol/POPS mixing ratio. The signal intensity at the Chol/POPS mixing ratio of 1.0 was used to normalize signal intensities at various other cholesterol contents. By rinsing test tubes with chloroform, it was confirmed that all cholesterol and all phospholipids were suspended in the buffer from the film on the test tube walls. No EPR signals from 5-PC or CSL were recorded in chloroform. However, the CSL signal intensity increased proportionally to the amount of cholesterol in the mixture, up to a Chol/POPS mixing ratio of 2.0–2.5, while the intensity of the 5-PC signal was the same up to a Chol/POPS mixing ratio of 3. Thus, the Chol/POPS molar ratio in the suspension (detected by EPR signals from 5-PC and CSL) was similar to the mixing ratio up to the Chol/POPS mixing ratio of 2.0–2.5 only.

3.2. Discrimination of the CBD in the Chol/POPS suspension

The existence of the CBD in all POPS suspensions when the cholesterol content exceeded the CST was confirmed by the EPR DOT method with the use of ASL [8,9]. The saturation-recovery signal of ASL measured for these membranes in the presence of oxygen is a double-exponential signal, which indicates that ASL molecules are located in two distinct environments, PCD and CBD, with different oxygen transport parameters (different oxygen diffusion-concentration products) (Fig.3A). As expected, the oxygen transport parameter in the CBD was significantly smaller than in the PCD. Although CSL data show a single value for the oxygen transport parameter for all cholesterol contents (data not shown), this does not mean that CSL detects a single homogeneous domain. Rather, this indicates that the collision rate between the nitroxide moiety of CSL and oxygen in both domains is the same. This statement was unambiguously confirmed by measurements with the water-soluble relaxation agent, NiEDDA, which showed that CSL is located in both domains (the PCD and CBD) and that these domains can be discriminated using the NiEDDA accessibility parameter (Fig.3B). As shown in Fig. 3B, the nitroxide moiety of CSL is more exposed to collisions with NiEDDA when CSL is located in the CBD and the nitroxide moiety is not hidden by the umbrella effect of the phospholipid headgroups (as in the PCD). These results are in agreement with polarity measurements for CSL and ASL (data not shown), indicating that the polarity around the nitroxide moiety of CSL increases when the cholesterol content increases beyond the CST. Polarity measurements also confirm that the nitroxide moiety of ASL is always located in the membrane center and is practically inaccessible for NiEDDA. The presence of cholesterol crystals in POPS membranes with high cholesterol contents (similar to those used in our work) was reported previously using DSC and X-ray diffraction methods [2,14–17].

The preexponential factors in the fitting of the saturation-recovery curves should indicate a population of ASL or CSL in the CBD and PCD. These factors, obtained for double-exponential saturation-recovery curves in the presence of oxygen (for ASL) and NiEDDA (for CSL), indicate that the distribution of cholesterol analogue spin labels between the CBD and PCD is close to the distribution of cholesterol. The preexponential factors that indicate the population of ASL in the CBD and PCD change from 0.46 and 0.52 (at a Chol/POPS ratio of 1) to 0.85 and 0.13 (at a Chol/POPS ratio of 3), respectively. The factors that indicate the population of CSL in the CBD and PCD change from 0.37 and 0.62 (at a Chol/

POPS ratio of 1) to 0.70 and 0.27 (at a Chol/POPS ratio of 3), respectively. The calculated distribution of cholesterol molecules between the CBD and PCD, assuming the CST is 0.5 and cholesterol forms only CBD and PCD domains, should change from 0.50 and 0.50 (at a Chol/POPS ratio of 1) to 0.83 and 0.17 (at a Chol/POPS ratio of 3), respectively. The preexponential factors are not robust parameters. They depend on the delay time after the saturating pulse ends, the number of cutting points during the fitting process, the exchange rate of spin labels between domains, and other conditions [29,35,37,38]. Therefore, we use the values mentioned above only to support our statement that cholesterol analogue spin labels behave similarly to the cholesterol in their distribution between the CBD and PCD.

3.3. Lipid-bilayer-like structure of the CBD

Figure 4 shows conventional EPR spectra for the phospholipid analogue 5-PC and the cholesterol analogues CSL and ASL in POPS-membrane suspensions recorded for different Chol/POPS mixing ratios. All spectra recorded for lipid suspensions up to the Chol/POPS ratio of 3 were characteristic for spin labels in lipid-bilayer-like structures. As expected, changes that occurred after the addition of cholesterol to the POPS membrane (up to its solubility threshold) reflect increased order of the phospholipid bilayer. In this situation, all spin labels are located in the phospholipid cholesterol bilayer. The CST in POPS membranes is 0.5 [14,21,25,26]. With this threshold and at a Chol/POPS mixing ratio of 2, about 75% of cholesterol molecules form the CBD and about 25% saturate the POPS bilayer forming the PCD. If this CST is exceeded, phospholipid analogue spin labels remain in the phospholipid cholesterol bilayer. However, ASL and CSL are distributed between the PCD and CBD. If we assume the distribution of cholesterol analogue spin labels is the same as the distribution of cholesterol (see Sect. 3.2), we can obtain EPR signals of ASL and CSL from the CBD by subtracting the signal obtained for the Chol/POPS mixing ratio of 0.5 (with a weight of 0.25) from the signal obtained for the Chol/POPS mixing ratio of 2 (see Fig.4). Changes in the spectra were evaluated with sets of spectral parameters, maximum splitting (a parameter related to the order parameter and indicating the amplitude of the wobbling motions of the long axes of the ASL and CSL molecules [39]), and the h_+/h_0 ratio (a parameter that considers both the orientation and rotational mobility of the ASL and CSL molecules [40]) (see the caption to Fig.4). In the above calculations, EPR signals from suspensions with a Chol/POPS mixing ratio of 2 were chosen as those with the greatest CBD component (see the “saturation” effect indicated in Fig. 2).

Our results allow us to conclude that in the CBD, ASL and CSL molecules are located in the lipid-bilayer-like environment. Differences in the spectral parameters, coming from the CBD and the PCD, lead us to conclude as well that in the CBD ASL and CSL molecules are better ordered and sense a slightly less-fluid environment than in the surrounding PCD bilayer. Maximum splitting values, however, are much smaller than those for rigid limit conditions (also mentioned in the caption to Fig. 4), which indicates that the lipid-bilayer-like structures of the CBD and PCD are fluid. These conclusions are supported by the saturation-recovery measurements of the T_1s of ASL and CSL, which change only slightly after formation of the CBD (data not shown). The T_1 value of the spin label in the deoxygenated sample depends primarily on the rate of motion of the nitroxide moiety within the lipid bilayer. Because the nitroxide moiety of both ASL and CSL is rigidly connected to the sterol ring structure, its orientation and motion reflect that of the rigid sterol ring. We can conclude that in the wide region of cholesterol content (up to a Chol/POPS mixing ratio of 2.0–2.5), when the CBD is formed, most of the cholesterol analogues (CSL and ASL) are located in the lipid-bilayer-like environment (I_{LB} value indicated in Fig. 2). Thus, the CBD, which is formed and detected with cholesterol analogue spin labels above the CST, exists as a cholesterol bilayer.

3.4. Suspensions made of pure cholesterol

To clarify why the CSL signal intensity in the membrane suspension does not reflect the total amount of cholesterol in the dry lipid film (I_X value indicated in Fig. 2), we repeated the experiments described in Sect. 3.1 for suspensions formed from pure cholesterol containing 1 mol% CSL. After removing the cholesterol suspension from the test tube, we rinsed the test tube walls with chloroform and recorded the EPR signal. The absence of a signal indicated that all CSL (and, thus, all cholesterol) was transferred to the suspension. The EPR signals recorded for all of the cholesterol suspensions (made from different amounts of cholesterol deposited as lipid film at the bottom of the test tube) consisted only of a single broad line, which is characteristic of spin labels with strong spin-spin interaction (Fig. 5A), without any evidence of the signal characteristic of CSL in the lipid-bilayer-like environment (as in Fig. 4). We compared this signal with that obtained for the dry film of cholesterol containing 1 mol% CSL before addition of the buffer (Fig. 5B). The signals were identical, which allows us to conclude that the cholesterol in the suspension is in the same form as in the dry film, which we call “solid-state aggregates”. Similar results were obtained when the dry film of cholesterol was formed from chloroform, ether, or pyridine cholesterol solutions. The evaporation process was very slow (a few days) to ensure formation of cholesterol crystals. Indeed, we confirmed using the DSC method that these cholesterol solid-state aggregates possess properties of cholesterol crystals. They showed clear transitions at 76°C, which indicated dehydration of the monohydrate form of cholesterol. On the second heating scan, transition occurred at 36°C, which can be attributed to the polymorphic phase transition of the anhydrous form. A significantly weaker transition occurred at 76°C (data not shown). In cholesterol solid-state aggregates, because of the spin-spin interactions between CSL molecules, the EPR signal is about five times broader than recorded for CSL in Chol/POPS suspensions (Fig. 4). This causes a significant decrease (~25 times) in the signal amplitude and explains why the broad signal is not observed in suspensions for low (lower than 3) Chol/POPS mixing ratios. The broad, single-line signal can be seen in Chol/POPS suspensions as a background signal, but only when the mixing ratio is very high, about 25 and greater (data not shown).

3.5. Effects of the CBD on the physical properties of the PCD

If the CBD is formed outside the PCD as a separate entity (Fig. 1B), its presence should not affect the properties of the separately existing PCD. However, when the CBD is formed as an integral part of the phospholipid bilayer and both domains coexist (Fig.1A and C), effects on the properties of the PCD are possible. To explo re these possibilities, we used strategies developed in studies of the effects of integral membrane proteins on properties of the bulk lipid bilayer [41,42] in which, using phospholipid spin labels with the nitroxide moiety attached at the C14 or C16 position, two-component EPR spectra were recorded, indicating the existence of phospholipids in the bulk bilayer and phospholipids in the boundary layer around integral membrane proteins. Thus, we used 14- and 16-PC with a goal to see a similar “boundary layer” of phospholipids around the CBD. EPR spectra of 14- and 16-PC in the investigated membrane suspensions did not show any components characteristic of the boundary layer (see Fig. 6 where the EPR spectra of 14- and 16-PC are presented for POPS membranes prepared from the Chol/POPS mixture with a mixing ratio from 0 to 3). However, these EPR spectra showed numerous changes in shape—as also occurred when the cholesterol content exceeded the CST. We characterized these spectral changes by the order parameter calculated as described previously [43]. The values used for calculation of the hydrocarbon chain order parameter were measured directly from EPR spectra, as indicated in Fig. 6. Results presented in Fig. 7A indicate that for POPS membranes the effect of cholesterol on the order parameter of 14- and 16-PC in the PCD is seen up to the Chol/POPS mole ratio of ~2, which exceeds four times the CST in POPS membranes (0.5,

as reported in Refs. [14,21,25,26]). Values of the order parameter for 5-PC (calculated based on EPR spectra presented in Fig. 4), which show the same trend, are also included in Fig.7A.

The order parameter is a static parameter that describes the amplitude of the wobbling motion of phospholipid alkyl-chains imposed by the membrane environment. In deoxygenated samples, the spin-lattice relaxation time (T_1) depends primarily on the rate of motion of the nitroxide moiety within the lipid bilayer and thus describes the dynamics of the membrane environment at the depth at which the nitroxide moiety is located [44]. Therefore, we completed our data with measurements of the membrane fluidity parameter that describe the dynamic membrane properties—namely, the spin-lattice relaxation time (T_1). It is clear from Fig. 7B that cholesterol increases the dynamics of the membrane center when its content is lower than the CST, which is manifested by the shorter T_1 of 16-PC. Further increase in cholesterol content causes a decrease in the dynamics of the membrane center, which is shown by longer T_1 values. For 14-PC, differences in the effect of cholesterol, below and above the CST, are less pronounced. Cholesterol did not change T_1 up to the CST. However, a significant increase in T_1 is shown at higher cholesterol contents. For 5-PC, increase in cholesterol content up to and beyond the CST causes increase in the T_1 value. The effect of cholesterol on membrane dynamics saturates at the Chol/POPS mole ratio of ~2.

Bach and Miller [45,46] showed that the number of water molecules bound to PS or PC molecules in membranes made from Chol/PL mixtures increases when CBDs are formed in the bilayer. This is explained by the presence of boundaries between the PCD (where phospholipids are located) and the pure CBD. Because the thickness of the CBD (34 Å [2,4,5,47]) is much smaller than the thickness of the PCD (40 to 42 Å for membranes saturated with cholesterol [7,48]), water accessibility to the polar headgroups of phospholipids, as well as to parts of hydrocarbon chains close to the polar headgroups, should increase at the boundary between the PCD and the CBD. We measured the local polarity around the nitroxide moiety of 5-PC in POPS membranes and showed that polarity increases sharply with an increase in the cholesterol concentration up to the solubility threshold. This result was expected because cholesterol increases membrane polarity up to the depth at which the steroid ring is immersed in the phospholipid bilayer [36]. However, polarity increases further when the cholesterol content increases beyond the CST, up to a Chol/POPS mixing ratio of 2 to 3 (Fig. 8A). Because our measurements of local polarity are performed for frozen samples, we confirmed these data by measuring the accessibility of the water-soluble relaxation agent NiEDDA to the nitroxide moiety of 5-PC at 25°C. As indicated in Fig. 8B, the NiEDDA accessibility parameter increases by ~20% when the cholesterol concentration reaches the solubility threshold and, additionally, increases by ~20% when the cholesterol content exceeds the solubility threshold. It is likely that at the boundaries between the PCD and the CBD the nitroxide moiety of 5-PC is more exposed to water and collisions with the water-soluble relaxation agent.

4. Discussion

The results presented here demonstrate that the CBD, which is formed in a lipid suspension when the cholesterol content exceeds the CST, has pronounced effects on the organization and dynamics of phospholipids in the PCD. The CBD increases the order of phospholipid alkyl chains and decreases their dynamics. The presence of the CBD also increases the polarity of the nearest headgroup region of the PCD and the accessibility of small, water-soluble molecules to that region. These findings are in agreement with both calorimetric [25] and X-ray diffraction data [21,26,49] on Chol/POPS mixtures, which show that the enthalpy of melting and interbilayer spacing continue to change after formation of the CBD (and cholesterol crystals) begins to take place (see also explanation in the end of the paper). Our

results and the cited literature [2,22–24,45,46] provide proof that the CBD is formed within the PCD as a coexisting domain and continues to exert influence on PCD structure and dynamics. Our results also demonstrate that the CBD, with the lipid-bilayer-like structure, is formed only in the presence of phospholipids in membranes made from mixtures with a Chol/POPS ratio up to ~2.

When the cholesterol content significantly exceeds a Chol/POPS ratio of ~2, cholesterol can be further suspended in buffer. However, the EPR signal of CSL from this suspension is significantly different than that from suspension formed for the Chol/POPS ratio below 2. This signal contains a broad, single-line component, which is identical with the signal obtained for the suspension of pure cholesterol. We conclude that the three-line EPR signals from CSL (as shown in Fig.4) characterize the fraction of cholesterol in the lipid-bilayer-like structures that is supported by POPS (in PCD and CBD), while broad, single-line signals (as shown in Fig. 5) characterize the fraction of cholesterol in solid-state aggregates, presumably outside the PCD and CBD. This broad, single-line signal is completely masked by the strong three-line signal at the Chol/POPS ratio close to 2 (see Sect. 3.4).

The only explanation of the appearance of the broad, single-line signal of CSL in solid-state aggregates of cholesterol is strong spin-spin interaction between CSL molecules. It is likely that during chloroform evaporation, due to differences in polarity and, thus, differences in cholesterol and CSL solubility in chloroform, the local concentration of CSL significantly increases as compared with the concentration of cholesterol. Cholesterol—because it is more polar—crystallizes first, leaving locally concentrated solutions of CSL that enhance spin-spin interaction and broaden the EPR signal. This broadening is not observed in the fraction of cholesterol that forms the CBD supported by the POPS. The observed broad, single-line signal of CSL suggests a different organization of cholesterol in these fractions, with a more rigid structure of solid-state aggregates. It is likely that cholesterol solid-state aggregates have the same structure as cholesterol crystals, as indicated in the literature [20,24]. Indeed, DSC measurements (Sect. 3.4) have shown characteristics of the presence of cholesterol crystal transitions in the suspension of cholesterol solid-state aggregates. We have shown that the EPR spin-labeling approach can discriminate the fraction of cholesterol that forms the CBD within the phospholipid bilayer from the fraction that forms cholesterol structures (cholesterol crystals) presumably outside the bilayer. Cholesterol analogue spin labels are superior probes for the structure and dynamics of the CBD. However, they are poor at detecting the organization of cholesterol molecules in cholesterol crystals.

Models created through molecular dynamics simulations (Dr. Marta Pasenkiewicz-Gierula, personal communication) allowed us to compare the organization and dynamics of cholesterol molecules in CBDs with those in PCDs and cholesterol crystals. Some characteristics of cholesterol molecules in the CBD are similar to those in cholesterol crystals (bilayer thickness, surface per cholesterol molecule), while others are similar to those in the PCD (tilt, molecular order parameter). Results showed that the CBD is a dynamic structure with cholesterol mobility similar to the PCD. This is the major difference compared with cholesterol crystals, where cholesterol molecules are immobile.

The only explanation of our results that will not contradict well-documented data from the literature is that when the cholesterol content in the phospholipid bilayer exceeds the CST, both the CBD and cholesterol crystals form in the membrane suspension (Fig. 1C). The former is detected by EPR spin-labeling methods, the latter by DSC as well as the X-ray diffraction and MAS NMR methods. The organization of cholesterol molecules in CBDs is similar to that in PCDs (the order and dynamics are similar as well) and different from the rigid structure of cholesterol crystals—although the bilayer structure of the CBD and the pseudo-bilayer structure of cholesterol crystals indicate certain structural similarities

between them. However, DSC clearly detects formation of cholesterol crystals and not CBDs, which are fluid cholesterol bilayers with water molecules that have unlimited access to cholesterol –OH groups. In this situation, dehydration of the monohydrate form of cholesterol to the anhydrous form (which, additionally, can stay in this form for a few hours) is not possible. It is difficult to evaluate fractions of cholesterol that form CBDs and cholesterol crystals. Our results show that in POPS membranes the CBD starts to form when the cholesterol content exceeds the solubility threshold and continues to form only to a Chol/POPS mixing ratio of about 2. Further increase in cholesterol content does not increase the amount of cholesterol in the form of the CBD. It is most probable that when the cholesterol content exceeds the CST, parts of cholesterol molecules also form cholesterol crystals.

Acknowledgments

This work was supported by grants EY015526, TW008052, EB002052, and EB001980 of the National Institutes of Health. The authors wish to thank Dr. Marta Pasenkiewicz-Gierula for many helpful discussions and sharing her MD simulation data with us.

References

1. Tulenko TN, Chen M, Mason PE, Mason RP. Physical effects of cholesterol on arterial smooth muscle membranes: evidence of immiscible cholesterol domains and alterations in bilayer width during atherogenesis. J Lipid Res. 1998; 39:947–956. [PubMed: 9610760]
2. Preston Mason R, Tulenko TN, Jacob RF. Direct evidence for cholesterol crystalline domains in biological membranes: role in human pathobiology. Biochim Biophys Acta. 2003; 1610:198–207. [PubMed: 12648774]
3. Borchman D, Cenedella RJ, Lamba OP. Role of cholesterol in the structural order of lens membrane lipids. Experimental eye research. 1996; 62:191–197. [PubMed: 8698079]
4. Jacob RF, Cenedella RJ, Mason RP. Evidence for distinct cholesterol domains in fiber cell membranes from cataractous human lenses. The Journal of biological chemistry. 2001; 276:13573–13578. [PubMed: 11278611]
5. Jacob RF, Cenedella RJ, Mason RP. Direct evidence for immiscible cholesterol domains in human ocular lens fiber cell plasma membranes. The Journal of biological chemistry. 1999; 274:31613–31618. [PubMed: 10531368]
6. Widomska J, Raguz M, Dillon J, Gaillard ER, Subczynski WK. Physical properties of the lipid bilayer membrane made of calf lens lipids: EPR spin labeling studies. Biochim Biophys Acta. 2007; 1768:1454–1465. [PubMed: 17451639]
7. Widomska J, Raguz M, Subczynski WK. Oxygen permeability of the lipid bilayer membrane made of calf lens lipids. Biochim Biophys Acta. 2007; 1768:2635–2645. [PubMed: 17662231]
8. Raguz M, Widomska J, Dillon J, Gaillard ER, Subczynski WK. Characterization of lipid domains in reconstituted porcine lens membranes using EPR spin-labeling approaches. Biochim Biophys Acta. 2008; 1778:1079–1090. [PubMed: 18298944]
9. Raguz M, Widomska J, Dillon J, Gaillard ER, Subczynski WK. Physical properties of the lipid bilayer membrane made of cortical and nuclear bovine lens lipids: EPR spin-labeling studies. Biochim Biophys Acta. 2009; 1788:2380–2388. [PubMed: 19761756]
10. Deeley JM, Mitchell TW, Wei X, Korth J, Nealon JR, Blanksby SJ, Truscott RJ. Human lens lipids differ markedly from those of commonly used experimental animals. Biochim Biophys Acta. 2008; 1781:288–298. [PubMed: 18474264]
11. Borchman D, Yappert MC, Afzal M. Lens lipids and maximum lifespan. Experimental eye research. 2004; 79:761–768. [PubMed: 15642313]
12. Rujoi M, Estrada R, Yappert MC. In situ MALDI-TOF MS regional analysis of neutral phospholipids in lens tissue. Analytical chemistry. 2004; 76:1657–1663. [PubMed: 15018564]
13. Estrada R, Puppato A, Borchman D, Yappert MC. Reevaluation of the phospholipid composition in membranes of adult human lenses by (31)P NMR and MALDI MS. Biochim Biophys Acta. 2010; 1798:303–311. [PubMed: 19925778]

14. Wachtel EJ, Borochov N, Bach D. The effect of protons or calcium ions on the phase behavior of phosphatidylserine-cholesterol mixtures. Biochim Biophys Acta. 1991; 1066:63–69. [PubMed: 1648395]
15. Borochov N, Wachtel EJ, Bach D. Phase behavior of mixtures of cholesterol and saturated phosphatidylglycerols. Chemistry and physics of lipids. 1995; 76:85–92. [PubMed: 7788803]
16. Epand RM. Cholesterol in bilayers of sphingomyelin or dihydrosphingomyelin at concentrations found in ocular lens membranes. Biophysical journal. 2003; 84:3102–3110. [PubMed: 12719240]
17. Cheetham JJ, Wachtel E, Bach D, Epand RM. Role of the stereochemistry of the hydroxyl group of cholesterol and the formation of nonbilayer structures in phosphatidylethanolamines. Biochemistry. 1989; 28:8928–8934. [PubMed: 2557911]
18. Knoll W, Schmidt G, Ibel K, Sackmann E. Small-angle neutron scattering study of lateral phase separation in dimyristoylphosphatidylcholine-cholesterol mixed membranes. Biochemistry. 1985; 24:5240–5246. [PubMed: 4074692]
19. Guo W, Hamilton JA. 13C MAS NMR studies of crystalline cholesterol and lipid mixtures modeling atherosclerotic plaques. Biophysical journal. 1996; 71:2857–2868. [PubMed: 8913623]
20. Loomis CR, Shipley GG, Small DM. The phase behavior of hydrated cholesterol. J Lipid Res. 1979; 20:525–535. [PubMed: 458269]
21. Bach D, Wachtel E. Phospholipid/cholesterol model membranes: formation of cholesterol crystallites. Biochim Biophys Acta. 2003; 1610:187–197. [PubMed: 12648773]
22. Epand RM. Preface. Biochim Biophys Acta. 2003; 1610:155–156.
23. Epand RM, Hughes DW, Sayer BG, Borochov N, Bach D, Wachtel E. Novel properties of cholesterol-dioleoylphosphatidylcholine mixtures. Biochim Biophys Acta. 2003; 1616:196–208. [PubMed: 14561477]
24. Epand RM, Bach D, Epand RF, Borochov N, Wachtel E. A new high-temperature transition of crystalline cholesterol in mixtures with phosphatidylserine. Biophysical journal. 2001; 81:1511–1520. [PubMed: 11509364]
25. Bach D. Differential scanning calorimetric study of mixtures of cholesterol with phosphatidylserine or galactocerebroside. Chemistry and physics of lipids. 1984; 35:385–392.
26. Bach D, Borochov N, Wachtel E. Phase separation of cholesterol from phosphatidylserine-cholesterol mixtures in the presence of the local anesthetic tetracaine. Chemistry and physics of lipids. 2004; 130:99–107. [PubMed: 15172826]
27. Bach D, Wachtel E. Thermotropic properties of mixtures of negatively charged phospholipids with cholesterol in the presence and absence of Li+ or Ca2+ ions. Biochim Biophys Acta. 1989; 979:11–19. [PubMed: 2917161]
28. Subczynski WK, Felix CC, Klug CS, Hyde JS. Concentration by centrifugation for gas exchange EPR oximetry measurements with loop-gap resonators. J Magn Reson. 2005; 176:244–248. [PubMed: 16040261]
29. Kawasaki K, Yin J-J, Subczynski WK, Hyde JS, Kusumi A. Pulse EPR detection of lipid exchange between protein rich raft and bulk domains in the membrane: methodology development and its application to studies of influenza viral membrane. Biophysical journal. 2001; 80:738–748. [PubMed: 11159441]
30. Subczynski WK, Hyde JS, Kusumi A. Oxygen permeability of phosphatidylcholine-cholesterol membranes. Proc Nati Acad Sci U S A. 1989; 86:4474–4478.
31. Yin JJ, Subczynski WK. Effects of lutein and cholesterol on alkyl chain bending in lipid bilayers: a pulse electron spin resonance spin labeling study. Biophysical journal. 1996; 71:832–839. [PubMed: 8842221]
32. Subczynski WK, Hyde JS. Concentration of oxygen in lipid bilayers using a spin-label method. Biophysical journal. 1983; 41:283–286. [PubMed: 6301572]
33. Hyde, JS.; Subczynski, WK. Spin-label oximetry. In: Berliner, LJ.; Reuben, J., editors. Biological Magnetic Resonance. Vol. 8. Plenum Press; New York: 1989. p. 399-425.
34. Subczynski WK, Antholine WE, Hyde JS, Kusumi A. Microimmiscibility and three-dimensional dynamic structures of phosphatidylcholine-cholesterol membranes: translational diffusion of a copper complex in the membrane. Biochemistry. 1990; 29:7936–7945. [PubMed: 2261449]

35. Subczynski, WK.; Widomska, J.; Wisniewska, A.; Kusumi, A. Methods in Molecular Biology, Lipid Rafts. Vol. 398. Humana Press; Totowa: 2007. Saturation-recovery electron paramagnetic resonance discrimination by oxygen transport (DOT) method for characterizing membrane domains; p. 143-157.
36. Subczynski WK, Wisniewska A, Yin J-J, Hyde JS, Kusumi A. Hydrophobic barriers of lipid bilayer membranes formed by reduction of water penetration by alkyl chain unsaturation and cholesterol. Biochemistry. 1994; 33:7670–7681. [PubMed: 8011634]
37. Ashikawa I, Yin J-J, Subczynski WK, Kouyama T, Hyde JS, Kusumi A. Molecular organization and dynamics in bacteriorhodopsin-rich reconstituted membranes: discrimination of lipid environments by the oxygen transport parameter using a pulse ESR spin-labeling technique. Biochemistry. 1994; 33:4947–4952. [PubMed: 8161556]
38. Subczynski WK, Wisniewska A, Hyde JS, Kusumi A. Three-dimensional dynamic structure of the liquid-ordered domain as examined by a pulse-EPR oxygen probing. Biophysical journal. 2007; 92:1573–1584. [PubMed: 17142270]
39. Kusumi A, Subczynski WK, Pasenkiewicz-Gierula M, Hyde JS, Merkle H. Spin-label studies on phosphatidylcholine-cholesterol membranes: effects of alkyl chain length and unsaturation in the fluid phase. Biochim Biophys Acta. 1986; 854:307–317. [PubMed: 3002470]
40. Schreier S, Polnaszek CF, Smith IO. Spin labels in membranes. Problems in practice. Biochim Biophys Acta. 1978; 515:395–436. [PubMed: 215206]
41. Griffith OH, Dehlinger PJ, Van SP. Shape of the hydrophobic barrier of phospholipid bilayers (evidence for water penetration in biological membranes). The Journal of membrane biology. 1974; 15:159–192. [PubMed: 4366085]
42. Ryba NJ, Horvath LI, Watts A, Marsh D. Molecular exchange at the lipid-rhodopsin interface: spin-label electron spin resonance studies of rhodopsin-dimyristoylphosphatidylcholine recombinants. Biochemistry. 1987; 26:3234–3240. [PubMed: 3038180]
43. Marsh, D. Electron spin resonance: spin labels. In: Grell, E., editor. Membrane Spectroscopy. Springer-Verlag; Berlin: 1981. p. 51-142.
44. Subczynski, WK.; Raguz, M.; Widomska, J. Studying lipid organization in biological membranes using liposomes and EPR spin labeling. In: Weissig, V., editor. Liposomes. Methods and Protocols. , vol. Volume 2:Biological Membrane Models. Humana Press; Glendale, AZ: 2010. p. 247-269.
45. Bach D, Miller IR. Hydration of phospholipid bilayers in the presence and absence of cholesterol. Biochim Biophys Acta. 1998; 1368:216–224. [PubMed: 9459599]
46. Bach D, Miller IR. Hydration of phospholipid bilayers in the presence and absence of cholesterol. Chemistry and physics of lipids. 2005; 136:67–72. [PubMed: 15941564]
47. Self-Medlin Y, Byun J, Jacob RF, Mizuno Y, Mason RP. Glucose promotes membrane cholesterol crystalline domain formation by lipid peroxidation. Biochim Biophys Acta. 2009; 1788:1398–1403. [PubMed: 19376082]
48. Lis LJ, McAlister M, Fuller N, Rand RP, Parsegian VA. Interactions between neutral phospholipid bilayer membranes. Biophysical journal. 1982; 37:657–665. [PubMed: 7074191]
49. Bach D, Borochov N, Wachtel E. Phase separation in dimyristoyl phosphatydilserine cholesterol mixtures. Chemistry and physics of lipids. 1998; 92:71–77.

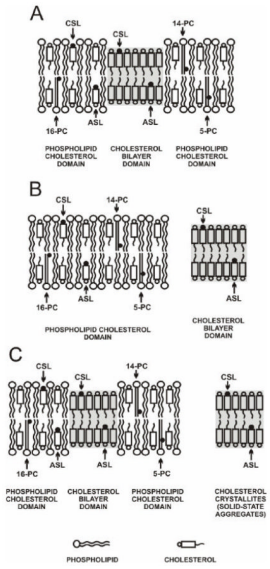

Fig. 1.

Schematic drawings of three possible cases for formation of the CBD domain: as an integral part of the phospholipid bilayer (A) and as a separate entity outside the PCD (B). The excess of cholesterol, which is not supported by the phospholipid bilayer as the CBD, can form ill-defined cholesterol structures (cholesterol crystals or solid-state aggregates) outside the membrane (C). The distribution and approximate location of lipid spin labels is indicated. Phospholipid spin labels (5-, 14-, and 16-PC) are only located in the PCD. However, spin-labeled cholesterol analogues (CSL and ASL) are distributed between both domains. The membrane used in this schematic drawing is made from POPS with a CST of 33 mol%. The nitroxide moieties of spin labels are indicated by black dots.

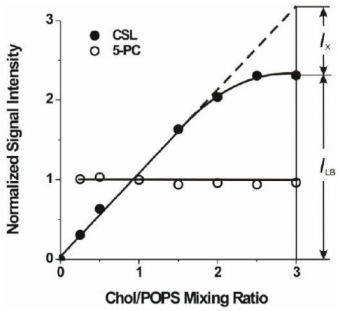

Fig. 2.

The normalized signal intensity for CSL (closed symbols) and 5-PC spin labels (open symbols) in Chol/POPS membranes plotted as a function of the Chol/POPS mixing ratio. I_{LB} indicates signal intensity for CSL in a lipid-bilayer-like environment (PCD and CBD), and I_X indicates "missing" signal intensity for CSL, which is not observed as a bilayer-like structure. The signal intensity was determined from a minimum of three measurements within accuracy better than ±10% for 5-PC and ±15% for CSL.

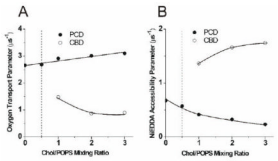

Fig. 3.

The oxygen transport parameter for ASL (A) and the NiEDDA accessibility parameter for CSL (B) in Chol/POPS membranes plotted as a function of the Chol/POPS mixing ratio. Values of these parameters in coexisting PCD and CBD are indicated.

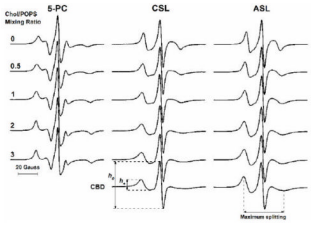

Fig. 4.

EPR spectra of 5-PC, CSL, and ASL in membranes made of Chol/POPS mixtures. Spectra were recorded at 25°C for different Chol/POPS mixing ratios. CBD indicates EPR spectra of CSL and ASL located in the CBD (see Sect. 3.3 for details of subtraction procedure). Maximum splitting values for CSL in PCD and CBD are 41.0 and 47.3 Gauss (the rigid limit is 70.0 Gauss), and for ASL in PCD and CBD, 39.1 and 43.2 Gauss (the rigid limit is 64.8 Gauss). Values of the mobility parameter h_+/h_0 for CSL in PCD and CBD are 0.26 and 0.22, and for ASL in PCD and CBD, 0.32 and 0.35. Measured values are indicated.

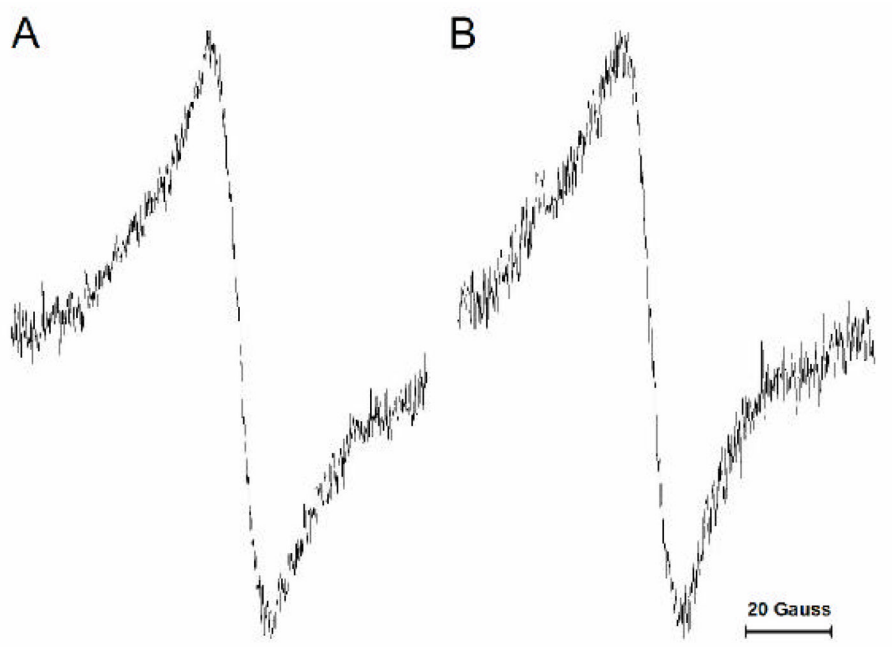

Fig. 5.

EPR spectra recorded for the suspensions formed from pure cholesterol containing 1 mol% CSL (A) and for the dry film of cholesterol containing 1 mol% CSL (B). Spectra were recorded at 25°C.

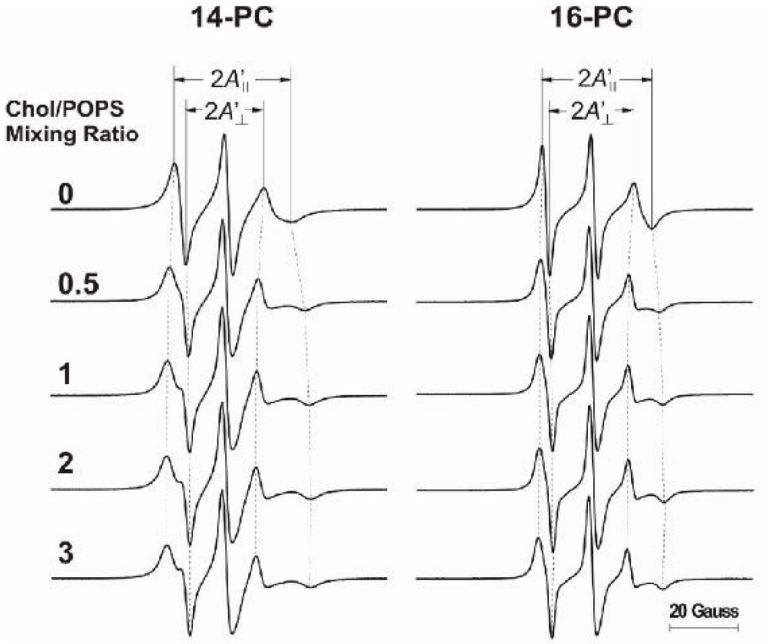

Fig. 6.

EPR spectra of 14- and 16-PC in membranes made of Chol/POPS mixtures. Spectra were recorded at 25°C for different Chol/POPS mixing ratios. The positions of certain peaks were evaluated with a higher level of accuracy by monitoring them at 10 times higher receiver gain and, when necessary, at higher modulation amplitude.

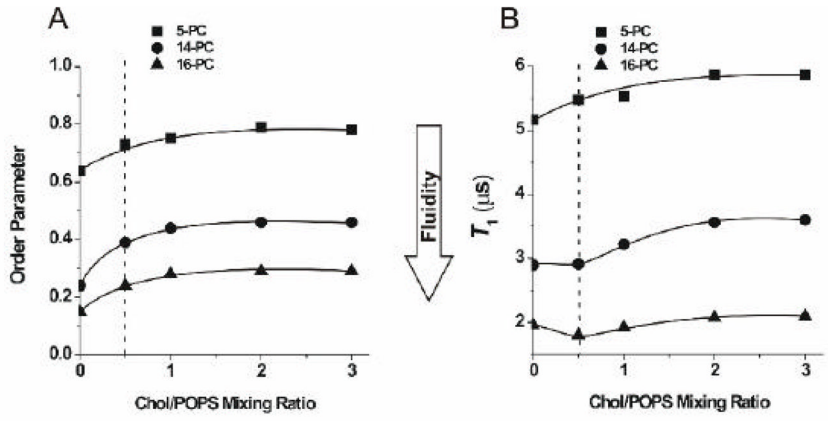

Fig. 7.

Order parameter of 5-, 14-, and 16-PC in Chol/POPS membranes plotted as a function of the Chol/POPS mixing ratio (A). Order parameters were calculated from spectra presented in Figs. 4 and 6. Because of the sharpness of the EPR lines and the method of measurements (see Fig. 6), A'_{II} and $A'_{\perp}$ values can be measured with the accuracy of ±0.1 G. Spin-lattice relaxation time (T_1) of 5-, 14-, and 16-PC in Chol/POPS membranes plotted as a function of the Chol/POPS mixing ratio (B). The decay time constants were determined from a minimum of three measurements within accuracy of ±3%. All measurements were performed at 25°C for deoxygenated samples. Broken lines indicate the CST in the POPS membrane.

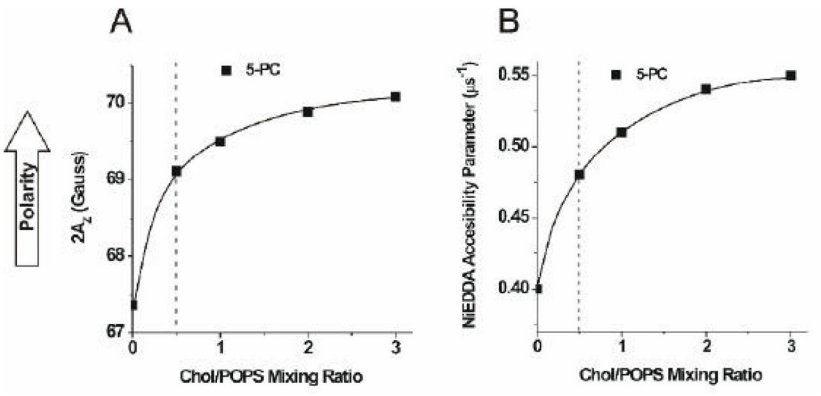

Fig. 8.

$2A_Z$ values for 5-PC in Chol/POPS membranes plotted as a function of the Chol/POPS mixing ratio (A). Upward changes indicate increase in polarity. The NiEDDA accessibility parameter for 5-PC in Chol/POPS membranes plotted as a function of the Chol/POPS mixing ratio (B). The NiEDDA accessibility parameter was determined from a minimum of three measurements within accuracy of ±3%. Broken lines indicate the CST in the POPS membrane.